

Modeling glow discharge at atmospheric pressure in argon

Abstract. This paper presents the characteristics of radio frequency atmospheric pressure discharge in argon based on numerical modeling. A fluid model with one-dimensional based on the first three moments of Boltzmann equation, coupled with Poisson's equations used in this work. The discharge usually consists of several locally filaments. The Radio-Frequency generator with an appropriate width and period, it was found possible to control the filament to glow transition in order to obtain diffused and stable plasma. The model allows us to obtain the axial distributions parameters of the discharge at different times of Radio-Frequency cycle (RF). The principal parameters are the electronic density, ionic density, electric potential, electric field and electronic temperature.

Streszczenie. W artykule przedstawiono charakterystykę wyładowań atmosferycznych o częstotliwościach radiowych w argonie na podstawie modelowania numerycznego. Model płynny z jednowymiarowym na podstawie pierwszych trzech momentów równania Boltzmana, w połączeniu z równaniami Poissona użytymi w tej pracy. Wyładowanie zwykle składa się z kilku lokalnych włókien. Stosując generator częstotliwości radiowej o odpowiedniej szerokości i okresie, okazało się możliwe kontrolowanie żarzenia do przejścia poświatowego w celu uzyskania rozproszonej i stabilnej plazmy. Model pozwala nam uzyskać parametry rozkładu osiowego wyładowania w różnych okresach cyklu częstotliwości radiowych (RF). **Modelowanie wyładowań w argonie przy ciśnieniu atmosferycznym.**

Słowa kluczowe: wyładowanie jarzeniowe pod ciśnieniem atmosferycznym, częstotliwość radiowa, DBD, model płynny.

Keywords: Atmospheric pressure glow discharge, Radio frequency, DBD, Fluid model.

Introduction

Atmospheric Pressure Glow Discharge controlled by dielectric barriers (APGD) plasma sources driven by a radio frequency (RF) power supply are developed to obtain non-equilibrium gas discharge plasmas with large area, high stability, uniformity and reactivity [1,2].

Recently, atmospheric pressure discharges have found several industrial and other applications such as thin film deposition, surface modification, ozone generation, sterilization, bio-decontamination and others. In principle, atmospheric pressure plasma devices can provide a crucial advantage over low-pressure plasmas because they eliminate complications introduced by the need for vacuum [3]. The benefit of their use lies in the fact that they offer the possibility of low production cost without the need for vacuum equipment. The dielectric barrier discharge (DBD) is a common plasma source used for these applications [2]. Most of atmospheric pressure discharges are dielectric barrier discharges (DBDs) operating in the kilohertz [4]. New sources running at much higher frequencies in the RF range are currently under investigation [1, 2, and 3].

Model formulation

In this work, the model used to describe the kinetics of the charged particles for the RF glow discharge at atmospheric pressure is the second order fluid model. It is based on the first three momentums resolution of the Boltzmann equation. These three moments are continuity, momentum transfer and energy equations, which are strongly coupled with the Poisson's equation by considering the local electric field approximation for ions and the local mean energy approximation for electrons. In the present model, the transport equations derived from the first three moments of Boltzmann's equation are written only for electrons and positive ions

$$(1) \quad \frac{\partial n_e}{\partial t} + \frac{\partial \Phi_e}{\partial x} = S_e$$

$$(2) \quad \frac{\partial n_+}{\partial t} + \frac{\partial \Phi_+}{\partial x} = S_+$$

where n_e , n_+ are the particle density electron and ion, Φ_e , Φ_+ are the particle flux electron and ion, S_e , S_+ are the source term accounting for loss and creation. Using the drift diffusion approximation, the transport of particles is

given by these equations

$$(3) \quad \Phi_e = -\mu_e n_e E - D_e \frac{\partial n_e}{\partial x}$$

$$(4) \quad \Phi_+ = +\mu_+ n_+ E - D_+ \frac{\partial n_+}{\partial x}$$

The transport coefficients of electrons as a function of the electric field and energy are calculated with BOLSIG+ [5]. In the source term, only the ionization is considered, and other reactions are neglected, because we think that ionization is the main process in the RF glow discharge [6, 7].

The source term S_e and S_+ are expressed as a function of the energy electron form as shown

$$(5) \quad S_e = S_+ = \alpha(\varepsilon_e) N n_e$$

The source term is obtained from the Townsend coefficient $\alpha(\varepsilon_e)$ tabulated as a function of the mean electron energy with BOLSIG+ [5].

The electron temperature is calculated by the energy electron equation given by

$$(6) \quad \frac{\partial n_e \varepsilon_e}{\partial t} + \frac{\partial \Phi_e}{\partial x} = S_e$$

where $n_e \varepsilon_e$ is the electron energy density and Φ_e is the electronic energy density flux.

The flux of electron energy density can be written as

$$(7) \quad \Phi_e = -\frac{5}{3} n_e \mu_e E - \frac{5}{3} D_e \frac{\partial n_e}{\partial x}$$

The source term S_e is represented by two terms, an ohmic heating term and a collision loss term given by

$$(8) \quad S_e = -e \Phi_e E - \sum_j S_j H_j$$

where the summation is over the reactions involving inelastic electron collisions and H_j is the electron energy

loss per collision. This summation included ionization and excitation. Where the term excitation is given by

$$(9) \quad S_{ex} = \alpha_{ex}(\varepsilon_e) N n_e$$

The relation between the electric field and the space charge in inter-electrode space is given by Poisson's equation

$$(10) \quad \frac{d^2V}{dx^2} = \frac{e}{\varepsilon_0 \varepsilon_r} (n_e - n_+)$$

where V is the electric potential, e is the elementary charge, ε_0 is the permittivity of free space and ε_r is the permittivity relative of dielectric barrier. The electric field axial E is found from the partial derivatives of the potential function, and are given by

$$(11) \quad E = -\frac{dV}{dx}$$

Boundary Conditions for the Plasma-Barrier Interfaces

The computational domains employed in this numerical study are presented in Fig.1.

The use of boundary conditions for the above mentioned transport equations are essential for the description of our problem.

In the model, boundary conditions were as follows:

At $x = 0$ (surface of left electrode)

$$(12) \quad V = V_{rf} \sin(2\pi ft)$$

At $x = d_1$ (surface of left dielectric)

$$(13) \quad \Phi_e = -\gamma \Phi_+$$

The total electron flux Φ_e coming out from the cathode barrier can be assumed to be equal to the sum of the secondary emission flux generated by incoming ions and electron desorption flux from the barrier

$$(14) \quad \frac{\partial n_+}{\partial x} = 0$$

$$(15) \quad T_e = T_{ec}$$

At $x = d_1 + d_g$ (surface of right dielectric)

$$(16) \quad \Phi_e = -\gamma \Phi_+$$

$$(17) \quad \frac{\partial n_+}{\partial x} = 0$$

$$(18) \quad T_e = T_{ec}$$

At $x = d_1 + d_g + d_2$ (surface of right electrode see fig. 1)

$$(19) \quad V = 0$$

Here γ is the secondary electron emission coefficient, V_{rf} is the peak radio-frequency voltage, d is the inter-electrodes spacing, d_1, d_2 are the distance left and the right dielectric, f is the excitation frequency.

At the plasma-barrier interfaces, all the incoming electron and ion fluxes Φ_e, Φ_+ toward the dielectric barriers

are assumed to be accumulated as surface charges on the barrier surfaces. Therefore, surface charge densities σ_e and σ_i can be calculated from [8]

$$(20) \quad \frac{\partial \sigma_e}{\partial x} = \Phi_e$$

$$(21) \quad \frac{\partial \sigma_i}{\partial x} = \Phi_i$$

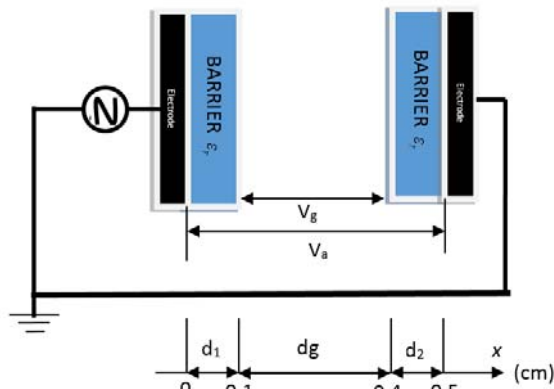


Fig. 1. Schematic diagram of the DBD simulation model for a parallel-plate reactor with double dielectric barriers

Numerical methods

Continuity equations

Scharfetter-Gummel exponential scheme is employed for the discretization of transport terms in the fluid model equations. This scheme is a special finite difference method [9]

$$\frac{n_i^{k+1} - n_i^k}{\Delta t} + \frac{\Phi_{i+1/2}^{k+1} - \Phi_{i-1/2}^{k+1}}{\Delta x} = S_i^k$$

$$\text{With: } \Phi_{i+1/2}^{k+1} = \frac{Y_{i+1}^{k+1} - Y_i^{k+1} \exp\left(\frac{w_{i+1/2}^k \Delta x}{D_{i+1/2}^{k+1}}\right)}{\frac{D_{i+1/2}^{k+1}}{w_{i+1/2}^k} \left(1 - \exp\left(\frac{w_{i+1/2}^k \Delta x}{D_{i+1/2}^{k+1}}\right)\right)}$$

$$w_{i+1/2}^k = \mu_{i+1/2}^k E_{i+1/2}^k, Y_{i+1}^{k+1} = n_{i+1}^{k+1} D_{i+1}^k,$$

$$E_{i+1/2}^k = -\frac{V_{i+1}^k - V_i^k}{\Delta x}, Y_i^{k+1} = n_i^{k+1} D_i^k$$

$$\Phi_{i+1/2}^{k+1} = \frac{(n_{i+1}^{k+1} D_{i+1}^k - n_i^{k+1} D_i^k \exp(T_1)) T_1}{\Delta x^2 (1 - \exp(T_1))}$$

$$T_1 = -s \frac{\mu_{i+1/2}^k}{D_{i+1/2}^k} (V_{i+1}^k - V_i^k)$$

The Poisson's equation (10) is most often discretized by using central finite-difference scheme

$$\text{With: } \frac{d^2V}{dx^2} = \frac{V_{i-1} - 2V_i + V_{i+1}}{\Delta x^2}$$

The resolution of the Poisson's equation is solved using iterative methods from the Successive Over-Relaxation (SOR) combined by Thomas algorithm for the tridiagonal matrix.

Results and discussions

This simulation is carried out at atmospheric pressure for a gas temperature 300 K. An voltage 1 kV is applied at left electrode (see Fig.1). The gas is subjected at 13.56 MHz excitation frequency, secondary electron emission coefficient is equal 0.1 are used as input parameters in this simulation [10]. The discharge gap width and thickness of dielectric barrier are 3 mm and 1 mm respectively. The dielectric constant of insulating barrier is assumed to be 10 in this modeling.

The table 1 present all the source data and the transport parameters used in our modeling.

Fig. 2 shows the electron and ion densities distribution in the gap for 25% and 75% of radio-frequency cycle. Electrons oscillate from one side of the gap to the other as the RF electric field oscillates. The ion density hardly varies during the cycle because of the low ionic mobility and the very rapid variation of the instantaneous electric field in the sheaths, which follows the movement of the electrons.

The transport of ions is therefore not sensitive to the temporal evolution of the electric field.

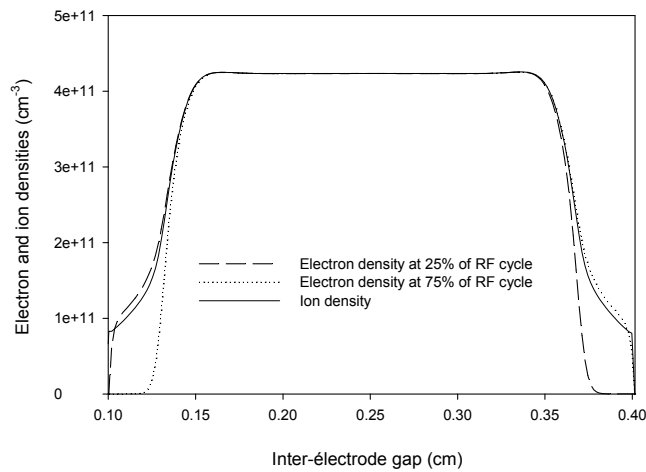


Fig. 2. Electron and ion densities at 25% and 75%RF cycle

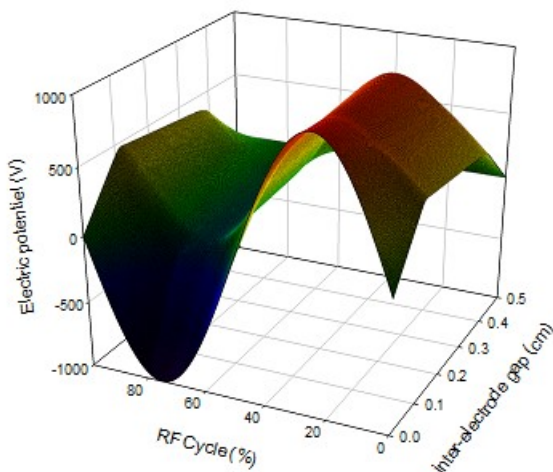


Fig. 3. Spatio-temporal distribution of the electric potential

The voltage applied to the left electrode creates a uniform electric field across the gap until the space charge created by charged particles of the plasma is high enough to modify the distribution of the electric field. The space resolved variation of the plasma potential is shown in Fig. 3 the potential on the right electrode is constant at 0 V.

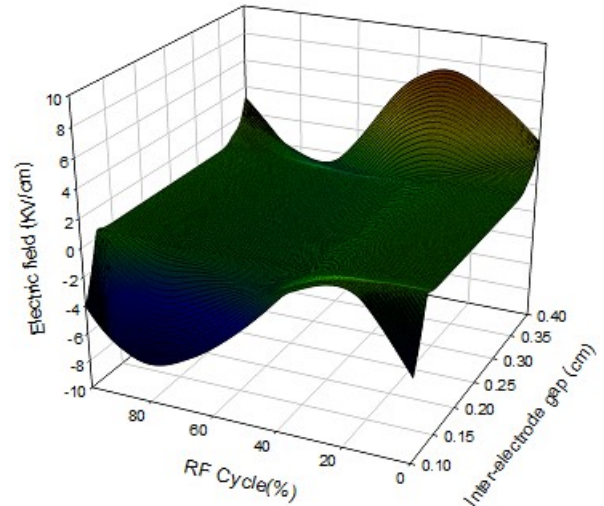


Fig. 4. Spatio-temporal distribution of the electric field

Fig. 4 shows the spatio-temporal variation of the electric field as a function of the position and the different moments of the cycle radiofrequency. The electric field is almost constant in the bulk of the plasma and it oscillates with a much greater amplitude in each sheath. In the bulk of the plasma the quasi-neutrality is respected and mainly assured by the balance between the electron density and the ion density. We can distinguish the three regions that characterize a glow discharge. A cathode fall characterized by relatively high electric field and positive ion density, positive column characterized by relatively low electric field and charge densities and the anode fall.

Fig. 5 shows the electron temperature distribution in the gap at 25% and 75% RF cycle. We observe much higher temperatures near the plasma-sheath interface during the cathodic part of the RF cycle, since the presence of the relatively intense electric field. In the plasma electron, temperature is lower and nearly time independent.

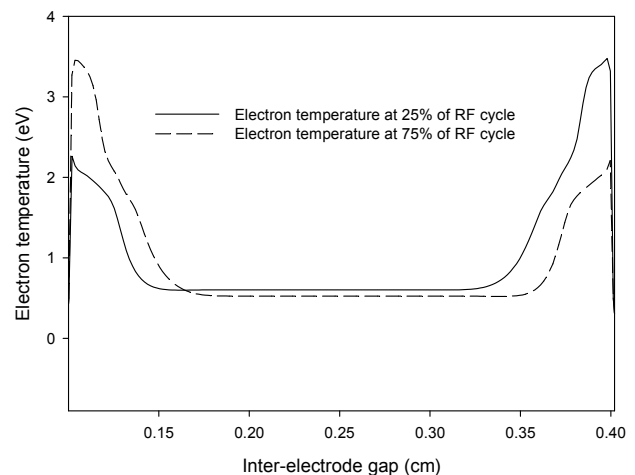


Fig. 5. Electron temperature on the symmetric axis at 25% and 75% RF cycle

The distribution spatio-temporal of heavy ions Argon is not affected by RF oscillations. As shown in Fig.6, their density remains steady regardless of the RF electric field variations.

The spatio-temporal profile of the electron density is shown in Fig. 7.

Table 1. Transport parameters and operating conditions used in the present simulation

Symbol	Value
$d(cm)$	0.5
$d_1(cm)$	0.1
$d_2(cm)$	0.1
$P(torr)$	760
$V_{rf}(KV)$	1
$f(MHz)$	13.56
$T_{gaz}(K)$	300
$ND_e(cm.s)^{-1}$	BOLSIG +
$ND_+(cm.s)^{-1}$	8.0×10^{17}
$N\mu_e(V.cm.s)$	BOLSIG +
$N\mu_+(V.cm.s)$	3.6×10^{19}
$\alpha_i(cm^3/s)$	BOLSIG +
$E_i(eV)$	15.7
$H_{ex}(eV)$	BOLSIG +
γ	0.5
$T_{ec}(eV)$	0.1

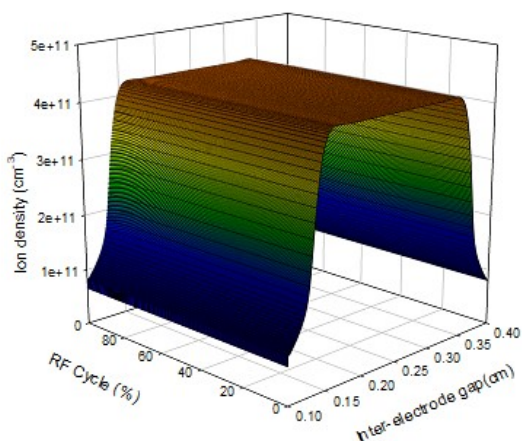


Fig. 6. Spatio-temporal distribution of ion density

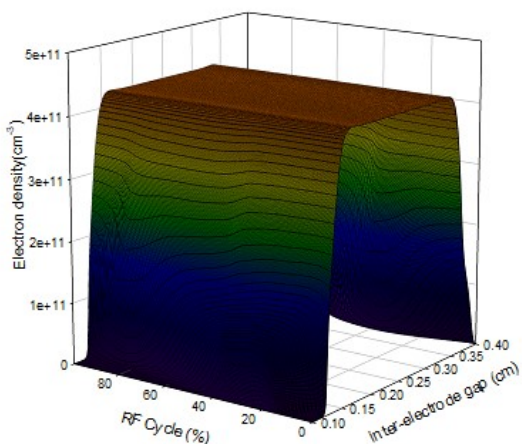


Fig. 7. Spatio-temporal distribution of the electron density

Conclusion

In this paper, the discharge characteristics of the atmospheric argon RF DBD plasmas generated at atmospheric-pressure DBDs are studied.

The one-dimensional fluid model with an energy equation for the electrons was written to gain insight into the glow discharge phenomena. It is based on the classical resolution of the fluid equations semi-implicitly coupled to Poisson's equation. The simulation of the spatio-temporal evolution of the plasma and of the argon kinetics allows a better interpretation and apprehension of the discharge physics.

The calculated results have been obtained for the temporal variations and spatial distributions of the discharge characteristics, such as electric field, electron density, and ion.

The atmospheric pressure RF discharge is similar to a lower pressure RF discharge for which the ionization occurs mainly inside the oscillating sheaths where electrons are the most energetic.

Nomenclature

n_e, n_+ and n_e	Electron, ion and energy number density
Φ_e, Φ_+	Electron and Ion flux
S_e, S_+ and S_e	Source term for electron, ion and energy
V	Electric potential
E	Electric field
ϵ_e	Electron energy
T_e	Electron temperature
μ_e, μ_+	Electron and Ion Mobilities
D_e, D_+	Electron and ion diffusion
γ	Coefficient for secondary electron emission
N	Neutral species density
e	Elementary charge
ϵ_0	Free space permittivity
ϵ_r	Dielectric permittivity
σ_e, σ_i	Surface charge densities
dg	Inter-electrode gap
Δx	Axial spatial step
Δt	Temporal step
T	Period

Authors

ZACH Tayeb Nasrallah was born in Oran, Algeria, on August, 27, 1989. His scientific interests include the theoretical study and modeling of physical processes in gas discharge plasma. E-mail: zach.tayeb@usto-univ.dz

Ali Hennad was born in Oran, Algeria, on January, 27, 1964. He received the PH.D degree with a thesis on the kinetics of ions in molecular gases to determine ion basic data in air from Monte Carlo simulation, University Paul Sabatier of Toulouse, France in 1996. He is currently a Professor at University of Sciences and Technology of Oran, Algeria. His field of expertise is more particularly the modeling of the electric and hydrodynamic behaviors of the plasmas generated in low and high pressure. He has also a good expertise on the numerical analysis of the nonlinear and strongly coupled elliptic transport equations, and the swarm parameters determination of the charged particles in no equilibrium reactive plasma. He is the author of various international publications, a lot of them in collaboration with the LAPLACE Laboratory, Toulouse, France. E-mail: ali.hennad@gmail.com

REFERENCES

- [1] Se Youn Moon, Choe W., and Kang B. K., A uniform glow discharge plasma source at atmospheric pressure, *Appl. Phys. Lett.* 84 (2004), No. 2, 188-190
- [2] Radu I., Bartnikas R., Czeremuszkin G., and Wertheimer M.R., Diagnostics of dielectric barrier discharges in noble gases: atmospheric pressure glow and pseudoglow discharges and spatio-temporal patterns, *IEEE Transactions on Plasma Science*, 31 (2003), No.3, 411-421
- [3] Shi J.J. and Kong M. G., Radio-frequency dielectric-barrier glow discharges in atmospheric argon, *Appl. Phys. Lett* 90 (2007), No. 2, 023306
- [4] Kogelschatz U., Eliasson B., Egli W., Dielectric-Barrier Discharges. Principle and Applications. *Journal de Physique IV Colloque*, 1997, 07 (C4), pp.C4-47-C4-66
- [5] BOLSIG+, electrons Boltzmann equation solver www.bolsig.laplace.univ-tlse.fr
- [6] Yu Qian, Deng Yong Feng, Numerical study on characteristics of argon radio-frequency glow discharge with varying gas pressure, *Chin.Phys.Lett.* 25 (2008), No. 7, 2569
- [7] Tebani H., Hennad A., Three-dimensional modelling of the DC glow discharge using the second order fluid model, *Przegląd Elektrotechniczny*, 89 (2013), nr. 8, 166-171
- [8] Woo Seok Kang, Jin Myung Park, Yongho Kim, and Sang Hee, Numerical study on influences of barrier arrangements on dielectric barrier discharge characteristics, *IEEE Transactions on Plasma Science*, 31(2003), No 4, 504-510
- [9] Scharfetter L., Gummel H.K., Large-signal analysis of a silicon Read diode oscillator, *IEEE Trans. Electron Devices*, 64 (1969), No.16, 64-77
- [10] Balcon N., Hagelaar G.J.M., and Boeuf J.P., Numerical Model of an Argon Atmospheric Pressure RF Discharge, *IEEE Transactions on Plasma Science*, 36 (2008), No. 5, 2782-2787